

RESEARCH

Open Access



The potential of novel arsenic nanoparticles containing metformin (MTF@As NPs): a study on their antioxidant and cytotoxic properties

Mojtaba Shakibaie^{1,2}, Seyed Soheil Hosseinasab³, Soudabe Riahi-Madvar¹, Mahboubeh Adeli-Sardou^{4*}, Fereshteh Jabari-Morouei⁵ and Hamid Forootanfar^{2,6*}

Abstract

In the present research, arsenic nanoparticles containing metformin (MTF@As NPs) were synthesized by subjecting a mixture of As_2O_3 and sodium borohydride solution to microwave irradiation in the presence of metformin. The physicochemical properties of the prepared nanoparticles were analyzed using UV-visible spectroscopy, Fourier transform infrared spectroscopy (FTIR), energy-dispersive X-ray spectroscopy (EDS), and scanning electron microscopy (SEM). The nanoparticles were assessed for their antioxidant potential, hemocompatibility, and cytotoxic effects. Based on the study's findings, it was found that MTF@As NPs have a size range of 14–38 nm. DPPH scavenging and iron-reducing assays demonstrated that MTF@As NPs exhibited significantly higher antioxidant activity than As NPs (80–1280 $\mu\text{g/mL}$). The study also revealed that nanoparticles were compatible materials that did not induce significant hemolysis in RBCs. According to the study, the concentration required for death of half of the cells (IC_{50}) treated with MTF@As NPs after 24 h was found to be $33.5 \pm 2.6 \mu\text{g/mL}$ and $5.7 \pm 0.3 \mu\text{g/mL}$ for MCF-7, and NIH3T3 cells, respectively. Notably, MTF@As NPs exhibited significantly higher toxicity against MCF-7 cells at higher concentrations (40–1280 $\mu\text{g/mL}$). This study provides insights into the cytotoxic properties of MTF@As NPs, additional investigation is necessary to fully understand these nanoparticles' underlying biological mechanisms.

Keywords Arsenic nanoparticles containing metformin, Antioxidant, Cytotoxicity, Hemolysis, Microwave irradiation

*Correspondence:

Mahboubeh Adeli-Sardou
m_adeli622002@yahoo.com
Hamid Forootanfar
h_forootanfar@kmu.ac.ir

¹Pharmaceutical Sciences and Cosmetic Products Research Center, Kerman University of Medical Sciences, Kerman, Iran

²Department of Pharmaceutical Biotechnology, Faculty of Pharmacy, Kerman University of Medical Sciences, Kerman, Iran

³The Student Research Committee, Faculty of Pharmacy, Kerman University of Medical Sciences, Kerman, Iran

⁴Department of Biotechnology, Institute of Science and High Technology and Environmental Sciences, Graduate University of Advanced Technology, Kerman, Iran

⁵Department of Food Science and Technology, Faculty of Agriculture Science and Research Branch, Islamic Azad University, Tehran, Iran

⁶Herbal and Traditional Medicines Research Center, Kerman University of Medical Sciences, Kerman, Iran

Introduction

The increasing prevalence of cancer and other oxidative stress-related diseases has necessitated the exploration of novel therapeutic agents that can effectively combat these health challenges. However, developing new cancer therapies presents numerous challenges, including the complexity of cancer biology and the heterogeneity of tumors. Additionally, high costs and lengthy clinical trials can delay the availability of new treatments. Researchers must also ensure that new therapies are safe and effective for diverse patient populations. Globally, breast and lung cancer are the most common cancer-related deaths. In more than half of breast cancer patients, metastases will occur to bones, livers, lungs, or brains [1, 2]. Among



© The Author(s) 2025. **Open Access** This article is licensed under a Creative Commons Attribution-NonCommercial-NoDerivatives 4.0 International License, which permits any non-commercial use, sharing, distribution and reproduction in any medium or format, as long as you give appropriate credit to the original author(s) and the source, provide a link to the Creative Commons licence, and indicate if you modified the licensed material. You do not have permission under this licence to share adapted material derived from this article or parts of it. The images or other third party material in this article are included in the article's Creative Commons licence, unless indicated otherwise in a credit line to the material. If material is not included in the article's Creative Commons licence and your intended use is not permitted by statutory regulation or exceeds the permitted use, you will need to obtain permission directly from the copyright holder. To view a copy of this licence, visit <http://creativecommons.org/licenses/by-nc-nd/4.0/>.

the various compounds being investigated, arsenic and its derivatives have garnered attention due to their multifaceted biological effects, particularly in oncology. Arsenic has historically been used in a variety of applications, including medicine, military, alloys, insecticides, and wood preservation. Arsenic (As), a metalloid element, exists in several allotropic forms, including elemental, sulfide, and carbonate, with common oxidation states of -3 , 0 , $+3$, and $+5$. Despite this, the use of arsenic for these applications is declining due to its toxicity [3]. Previous studies have demonstrated the potential of arsenic-containing compounds to exhibit antibacterial, antiparasitic, antiviral, and anti-cancer activities [4]. As⁺³ ions can readily bind to protein residues, potentially leading to a depletion of intracellular glutathione. Conversely, As⁺⁵ ions have been shown to compete with phosphate in the citric acid cycle, which may disrupt the process of ATP synthesis [5]; arsenic trioxide (ATO) has a long history of use as both a poison and a drug, spanning over two thousand years. Since its introduction as a frontline treatment option for acute promyelocytic leukemia (APL), this treatment has drastically improved the survival rates of patients, transforming APL into a curable disease in a time and dose-dependent manner [6]. Arsenic trioxide (ATO) has demonstrated efficacy as a chemotherapeutic agent in various malignancies [7]. However, ATO can cause side effects such as hyperleukocytosis, liver and kidney dysfunction, and effusion. Due to the limitations associated with traditional arsenic-containing compounds and their various side effects, there has been a growing interest in developing novel arsenic-based compounds or alternative administration procedures that can help mitigate these side effects [8].

Nanomedicine is an area of medicine that uses nanotechnology to diagnose, treat, and prevent diseases. As well as imaging, diagnosis, cancer therapy, drug and gene delivery, immunotherapy, and tissue engineering, nanomaterials have been used to develop new drug delivery systems that target specific cells or tissues in medicine and pharmaceuticals [9]. Nanoparticles' unique potentials such as drug encapsulation, enable them to more effectively deliver medications by binding to specific targets. This selectivity can enhance bioavailability and lessen medication toxicity [10]. Additionally, nanoparticles (NPs) are now providing advantages in the field of therapeutics, particularly in terms of drug stability and easier surface modification [11]. nanoparticles have also drawn much interest in their anti-inflammatory, antioxidative, antiangiogenic, antiproliferative, and antidiabetic potentials [12]. Researchers believe these small-scale particles could enhance efficacy while causing less systemic toxicity throughout the body.

The substantial adverse effects of arsenic metal oxides, such as arsenic trioxide (ATO), limit its therapeutic

usage. Through recent advancements in nanotechnology, As-containing nanoparticles (NPs) have been developed with different sizes and structures from the parent molecules, which can enhance bioavailability and target delivery of medicines [13]. As NPs trigger apoptosis through various mechanisms. For example, they alter the balance of reactive oxygen species (ROS), suppress oncogenic genes, and induce proapoptotic-related genes [14]. Studies have demonstrated that As containing NPs induce cytotoxic effects on a range of cancer cell lines, such as breast cancer (MCF-7 and MDA-MB-231) [13], lung cancer (A549) [15], APK [16] (NB4), Glioblastoma (U251) [17], and hepatocellular carcinoma (Huh7 and HepG2) [18] efficiently. Encapsulation of As₂O₃ in nanostructures such as dual oligopeptides-conjugated nanoparticles containing As₂O₃ [19], thiolated chitosan nanoparticles containing As₂O₃ [20], apoferritin nanocage containing arsenoplatin [21], and PLGA/arsenic trioxide nanoparticles have been used to increase the efficacy of arsenic against cancer cells [22]. Recent research has demonstrated the efficacy of As₂O₃-loaded poly(lactide-co-glycolide) (PLGA) nanoparticles in enhancing targeted delivery to SMMC-7721 cells while simultaneously reducing cytotoxic effects on normal human liver cells (LO2 cells), which in vivo analysis further revealed that these nanoparticles exhibited no toxic effects on liver and kidney function, while significantly inhibiting liver tumor growth [23]. In a study published by Yin et al. in 2014, a novel nanoparticle-based delivery system for As₂O₃ that targeted hepatocellular carcinoma (HCC) cells was developed. The nanoparticle system consisted of As₂O₃ encapsulated in stealth nanoparticles conjugated with a single-chain variable fragment (ScFv) antibody that specifically recognized the vascular endothelial growth factor receptor-2 (VEGFR-2), which is highly expressed in HCC cells. Their research showed that nanoparticles inhibit HCC cell growth, reduce angiogenesis, and suppress tumor growth. The anti-angiogenic effects of the nanoparticles, in addition to their direct cytotoxic effects on cancer cells, may have contributed to their overall therapeutic efficacy [24].

Metformin (MTF), a traditional anti-hyperglycemic agent utilized in managing type 2 diabetes mellitus, is widely prescribed due to its favorable safety and tolerability profile [25]. Its hypoglycemic effect is mediated through the suppression of hepatic gluconeogenesis [26]. Recent investigations have elucidated additional benefits of metformin. For example, a study by Pedrosa et al. reported that MTF administration is associated with reduced mortality risk, decreased hospitalization and ICU admission requirements, and lower mortality rates in patients diagnosed with COVID-19 [27]. Furthermore, Seylan et al. showed that MTF increases the lifespan of fission yeast by modifying energy metabolism and stress

response pathways [28]. Many cytological studies have confirmed metformin's ability to inhibit cell proliferation and induce apoptosis in breast, prostate, pancreatic, lung, cervical, and liver tumor cells [29, 30].

For instance, Wu et al., have shown that MTF amplifies cell death mechanisms, particularly apoptosis, in a broad spectrum of cancer cells [31]. Furthermore, synergistic anti-cancer effects of MTF with different compounds such as doxorubicin [32], carboplatin [33], resveratrol [34], Lenvatinib [35], and arsenic trioxide [30, 36, 37] have been previously reported. With the above-mentioned considerations, this study aimed to develop a new, rapid, and simple method for synthesizing MTF@As nanoparticles (MTF@As NPs). After characterization, the antioxidant properties, hemocompatibility, and cytotoxicity of the prepared NPs were assessed through various biological tests. We hope to gain insight into the potential clinical applications of MTF@As NPs by further investigations.

Materials and methods

Chemicals

All chemicals utilized in this study were purchased from Sigma Company (St. Louis, MO, USA) and included metformin, sodium borohydride, Arsenic (III) oxide (As_2O_3), and 3-(4, 5-dimethylthiazol-2-yl)-2, 5-diphenyl-2 H-tetrazolium bromide (MTT). Additional reagents, including $\text{Na}_2\text{HAsO}_4 \cdot 7\text{H}_2\text{O}$, 2,2-diphenyl-1-picrylhydrazyl (DPPH), Ascorbic acid, sodium dihydrogen phosphate (NaH_2PO_4), disodium hydrogen phosphate (Na_2HPO_4), potassium ferricyanide, sodium carbonate (Na_2CO_3), trichloro acetic acid (TCA), sodium citrate, dextrose, citric acid, and ferric chloride (FeCl_3) were provided by Merck (Germany). Borna Pouyesh Gene Company (BPGene Co., Kerman, Iran) supplied fetal bovine serum, trypsin, and DMEM medium.

Ethical approval

The ethical committee of the Kerman University of Medical Sciences approved this study (Ethical approval Code: IR.KMU.REC.1400.675).

Preparation of nanoparticles

To synthesize MTF@As NPs, 50 μL of metformin solution (50 mM) was added to 8 mL of As_2O_3 solution (1 mM, in 1% w/w NaOH). The mixture was then transferred to a microwave oven after adding 7 mL of water and 300 μL of ice-cold sodium borohydride solution (1 mM). After five irradiation cycles (each cycle containing 10 s of microwave irradiation at 850 W and 30 s of rest outside the microwave), the mixture's color shifted to dark brown. The suspension was centrifuged at 12,000 rpm for 25 min. After washing with water, the final plate was dispersed in water and stored in the 4 °C

refrigerator. The arsenic nanoparticles were prepared in the same way without the presence of metformin. The stock of NPs was autoclaved for 20 min at 200 kPa and 121 °C then stored at 4 °C for use in the following steps.

Characterization of NPs

A variety of methods and devices were used to characterize As NPs and MTF@As NPs. Metformin, As NPs, and MTF@As nanoparticles were studied using UV-Vis between 200 and 600 nm. A Zeiss 902 A scanning electron microscope was used to capture SEM images of the NPs, and an energy-dispersive X-ray (EDX) microanalyzer was used for elemental analysis. A drop of MTF@As nanoparticles suspension was placed on carbon-coated copper TEM grids and dried under an infrared lamp. TEM analysis was carried out using a TEM microscope (model EM 400, FEI- Philips/FEI, Eindhoven, the Netherlands) operated at an accelerating voltage of 80 kV. The particle size distribution patterns were evaluated by counting 400 NPs on each TEM micrograph. Particle size distribution patterns of nanostructures were also determined by laser light scattering method using a Zetasizer MS2000 (Malvern Instruments, Malvern, UK). The FTIR spectrum of oven-dried NPs was obtained in the 400–4000 cm^{-1} range using a Nicolet™ iS20 FTIR spectrophotometer. Analyses were quantitatively carried out using spectrophotometry. First, the absorbance at 232.5 nm of water-dissolved metformin was plotted against different concentrations of metformin (0.5–80 $\mu\text{g mL}^{-1}$). Thereafter, the freshly prepared suspension of MTF@As nanoparticles was centrifuged (12,000 rpm, 25 min), and UV absorbance of the supernatant was determined at 232.5 nm against the supernatant of freshly prepared As NPs suspension prepared with the same method without using the metformin. In this study, NPs were prepared over three days, and the procedures were conducted in triplicate. It was determined that the amount of metformin on the surface of the NPs was determined using the mean of the measured absorbance following the measurement of the dry weight of MTF@As (50 °C, 48 h).

Evaluating the antioxidant properties of NPs

DPPH scavenging activity

The radical scavenging capacity of MTF@As NPs, As NPs, and Ascorbic acid in aqueous media was determined by modifying the previous procedure [38]. Different concentrations of NPs (0–1280 $\mu\text{g/mL}$) were mixed with 150 mL of DPPH solution (1 mM). Incubation in the dark at room temperature for 30 min was followed by measurement of the absorbance at 517 nm. Deionized water and Ascorbic acid solutions (0–1280 $\mu\text{g/mL}$) were used as positive and negative controls, respectively. Using the following formula, we calculated the percentage of DPPH scavenging activity:

$$\text{DPPH scavenging effect (\%)} = [1 - (A_a - A_b) / A_c] \times 100 \quad (1)$$

A_a is the absorbance of the sample mixed with DPPH, A_b is the absorbance of the sample without DPPH, and A_c is the absorbance of the control solution.

Reducing power assay

An improved version of a previously described technique was used to determine the reducing power of the NPs [39]. In this procedure, 500 μL of NP solutions (0–1280 $\mu\text{g}/\text{mL}$) were combined with 250 μL of w/v potassium ferricyanide (1%) and 250 μL of sodium phosphate buffer (0.2 M). After 20 min at 65 $^\circ\text{C}$, the mixture was added to 1 mL of (10% w/v) TCA solution and centrifuged for 15 min at 3000 rpm. The supernatant was added to 100 μL of deionized water and 20 μL of 6 mM FeCl_3 . The absorbance of the samples was determined at 700 nm. Ascorbic acid solutions (0–1280 $\mu\text{g}/\text{mL}$) were considered as a control. A plot was generated using the average absorbance values of three experiments conducted in triplicate.

In vitro hemolytic assay

A method developed by Satarzadeh was used to assess the hemolytic properties of the nanoparticles [40]. After collecting and heparinizing the whole blood cells, they were centrifuged at 3000 rpm for five minutes at room temperature. Using Alsever's solution (0.1116 M dextrose, 0.071 M sodium chloride, 0.027 M sodium citrate, and 0.002 M citric acid), RBC pellets were washed three times and diluted in a ratio of 1:10. The prepared cell

suspension was incubated at 37 $^\circ\text{C}$ for 30 min with an equal volume of NPs at concentrations ranging from 0 to 2560 $\mu\text{g}/\text{mL}$. After centrifuging the supernatant for four min at 3000 rpm, the supernatant was collected. Deionized water and Alsever's solution were used as controls (100% hemolysis and 0% hemolysis, respectively). At a wavelength of 415 nm, the absorbance of the samples was determined. We repeated the experiment three times on different days and calculated the percentage of hemolysis (HP) by using the following formula:

$$\text{HP (\%)} = \left[\frac{A_s - A_n}{A_p - A_n} \right] \times 100 \quad (2)$$

Where A_s is the absorbance of the experimental group, A_n is the absorbance of the negative control group, and A_p is the absorbance of the positive control group.

Cytotoxicity test

The MCF-7 breast cancer cell line and mouse embryonic fibroblast cells (NIH3T3) were obtained from the Iranian Biological Resource Center. The cells were seeded in a 96-well plate during the logarithmic growth phase. Various concentrations of NPs and As_2O_3 solution were added. The medium was replaced after 24 h with MTT solution and incubated for 3 h. After replacing the medium with DMSO, the optical density was determined. The IC_{50} values were calculated by GraphPad Prism 9 software using non-linear regression analysis. Results are expressed as mean \pm SD.

Statistical analysis

One-way ANOVA was used to analyze the results of the experiments by the software SPSS 25 (SPSS Inc., Chicago). A p -value of less than 0.05 was considered statistically significant. Three different experiments were performed for each experiment.

Result and discussion

Fabrication and characterization of NPs

NaBH_4 was combined with metformin and the microwave method to prepare metformin-coated arsenic nanoparticles (MTF@As NPs). Figure 1a and b illustrate the mixture of aqueous arsenic trioxide, metformin solution, and sodium borohydride before and after heating in a microwave oven (50 s, 850 W). A cloudy, dark brown mixture resulted from reducing As^{3+} ions to NPs. The arsenic trioxide solution exhibited its absorbance band at 217 nm according to UV-VIS spectroscopy (Fig. 1c). The peak was not observed after the microwave radiation. The UV-VIS spectroscopy of metformin is shown in Fig. 1d. The formation of arsenic nanoparticles resulted in a broad absorption near 260 nm (Fig. 1e). Furthermore, MTF@As nanoparticles showed a peak at 232 nm

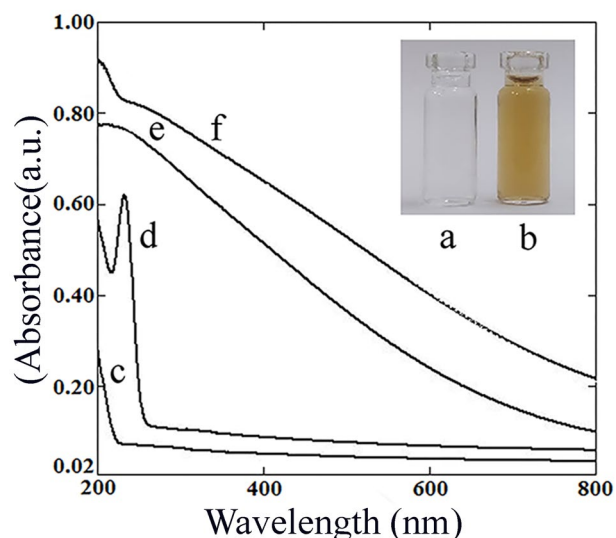


Fig. 1 The reaction mixture's color, consisting of arsenic trioxide, metformin solution, and sodium borohydride, was observed before (a) and after (b) being heated in a microwave oven. The UV-Vis absorption spectra for (c) arsenic trioxide, (d) metformin, (e) As NPs, and (f) MTF@As NPs were synthesized by the microwave oven

(Fig. 1f). In previous study, Pal et al. demonstrated that yellowish-brown spherical As NPs (45 nm) prepared by a wet chemical method exhibit a broad absorption peak in the UV-visible region between 250 and 350 nm without any individual peak [41].

MTF@As NPs synthesized by microwave-assisted synthesis showed a peak in the size range of 14 to 38 nm, with the 18 nm size being most frequent (Fig. 2a). In addition, as NPs showed a single peak in the size range of 16 nm to 45 nm, with the most frequent NPs being 19 nm (data not shown). Previously Kalyan et al. found that the size of As NPs, prepared by a chemical method at 10 °C and 40 °C, was 50 nm and 70 nm, respectively [42]. According to another study, *Escherichia coli* was used to synthesize 20–30 nm As NPs by constructing a modular arsenic resistance operon [43]. The SEM provided additional information on the morphology and shape of MTF@As nanoparticles (Fig. 2c). The SEM micrograph revealed that the nanoparticles had formed larger particles as they interconnected with each other. The related

TEM micrograph and the particle size distribution patterns are shown in Fig. 2b, and 2d.

The EDX profile of the MTF@As NPs displayed peaks of As L α at 1.28 KeV, which was related to the presence of arsenic in the prepared nanoparticles (Fig. 3). In the study of Balaz et al., the existence of arsenic with a similar value of As L α (1.28 KeV) has been reported in the EDX spectrum of arsenic sulphide nanoparticles (21–31 nm) [39]. In another study, amorphous arsenic sulphide nanoparticles with a size range of 50–200 nm were synthesized by a shallow water hydrothermal method, exhibiting a similar As L α peak at 1.28 keV [40]. Other related peaks of carbon K α (1.28 KeV) and nitrogen K α (0.52 KeV), which were observed in the EDX spectrum (Fig. 3), could be related to the metformin in the structure of nanoparticles.

Several absorption peaks in various spectrum regions of MTF@As NPs and metformin were determined by FTIR analysis (Fig. 4). The FTIR spectra of NPs synthesized at different times do not exhibit any significant

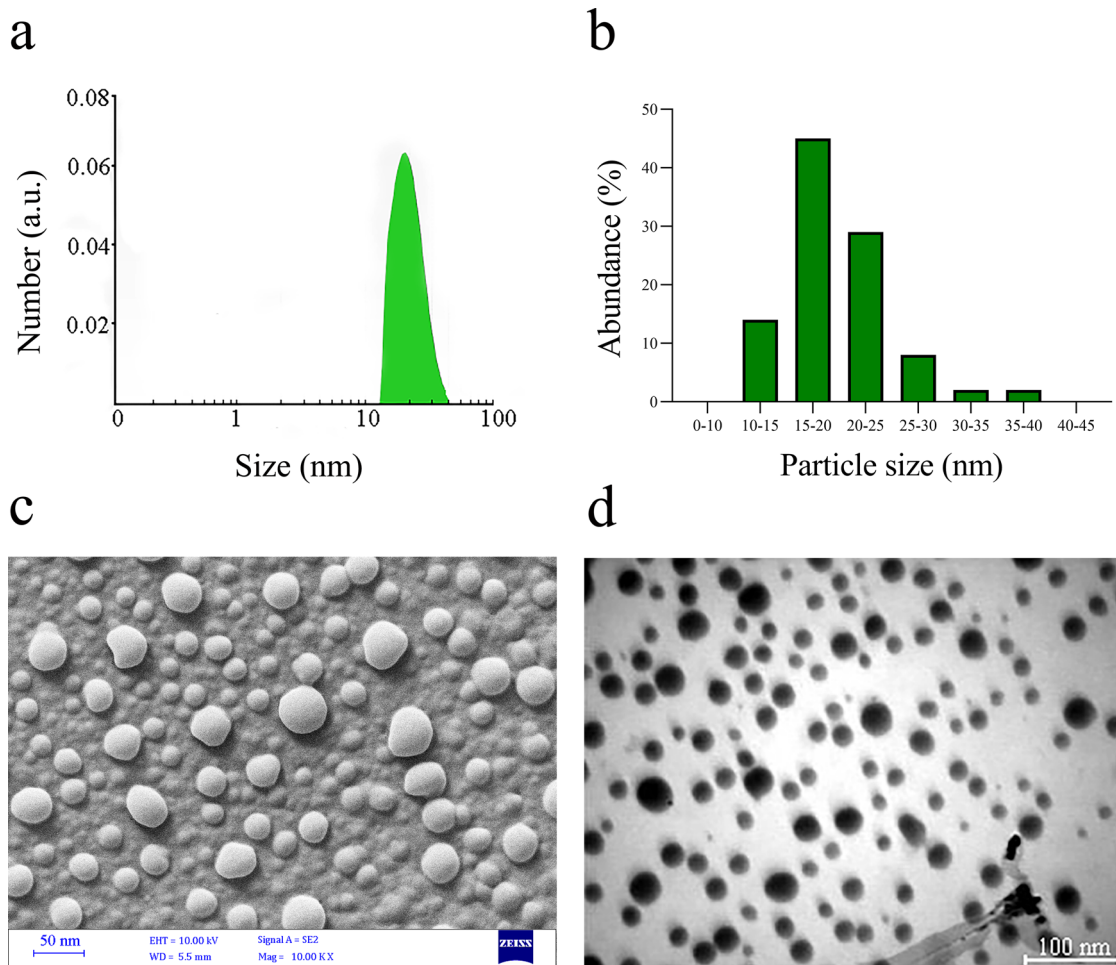


Fig. 2 (a) The particle size distribution pattern determined by laser light scattering method using a Zetasizer MS2000, (b) particle size distribution by counting 400 NPs on each TEM micrograph, (c) The spherical shape of MTF@As nanoparticles revealed by SEM micrograph, and (d) The spherical shape of MTF@As nanoparticles revealed by TEM micrograph

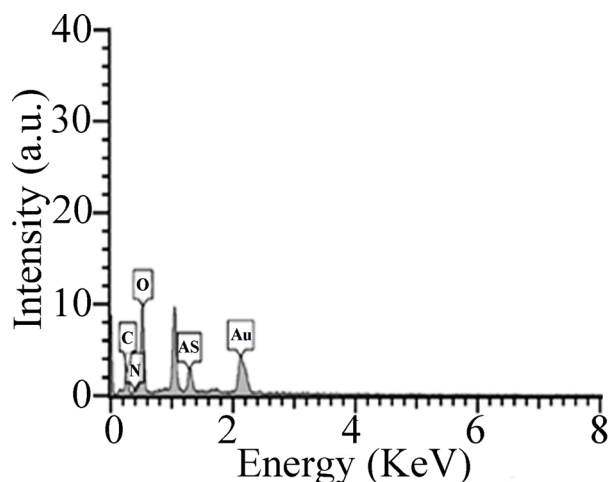


Fig. 3 EDX analysis of MTF@As nanoparticles

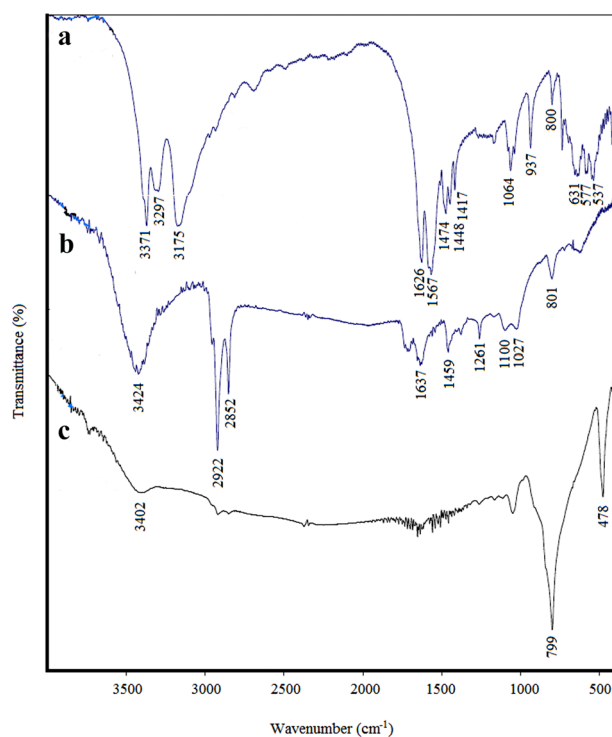


Fig. 4 Fourier transforms infrared (FTIR) absorption spectra of (a) Metformin, (b) MTF@As NPs, and (c) As NPs

differences (data not shown). The FT-IR spectrum of pure metformin hydrochloride showed characteristic bands at 3371 cm^{-1} , 3297 cm^{-1} , 3174 cm^{-1} , 1626 cm^{-1} , 1474 cm^{-1} , 1448 cm^{-1} , 1417 cm^{-1} , 1064 cm^{-1} , and 800 cm^{-1} , which are ascribed to an amine N-H group (first N-H stretching), amine N-H group (asymmetric N-H stretching), symmetric N-H stretching, N-H deformation, symmetric N-H deformation, N-H deformation, N-H deformation, C-N stretching of a secondary amine, and NH_2 rocking, respectively (Fig. 4a). In the FT-IR spectrum of MTF@As NPs (Fig. 4b), different peaks were detected at

3424 cm^{-1} , 2922 cm^{-1} , 2852 cm^{-1} , 1637 cm^{-1} , 1459 cm^{-1} , 1261 cm^{-1} , 1100 cm^{-1} , 1027 cm^{-1} , and 801 cm^{-1} . These were ascribed to an O-H group, C-H stretching band, C-H stretching band, C=N stretching band, C-H bending (which could also be for 1261 cm^{-1} and 1100 cm^{-1}), C-N stretching of a secondary amine, and C-H band, respectively. The FTIR spectrum of As NPs is depicted in Fig. 4c.

Microwave-assisted synthesis combined with “Green” methods for preparing nanostructures enabled the addition of different chemical functional groups to the surfaces of the nanoparticles [44]. The study of Ameri et al., which used sodium alginate (as a stabilizer agent) and Ascorbic acid (as a reducing agent) for microwave-assisted biosynthesis of palladium nanoparticles, reported that FTIR spectra demonstrated that the functional group of Ascorbic acid could play a role in the synthesis of Pd nanoparticles [45]. Additionally, Shakibaie et al., who used an aqueous extract from *Eucalyptus camaldulensis* for the fabrication of Pt nanoparticles through microwave irradiation, reported a similarity between the FTIR spectra of dry extract and prepared Pt nanoparticles, resulting from the attachment of different compounds in the extract to the surface of the Pt nanoparticles during the formation process [46]. In the present study, there are similarities between the metformin and MTF@As NPs in the fingerprint region of the FTIR spectrum (400 cm^{-1} – 3500 cm^{-1}). The diagnostic peaks of metformin exhibited in the FT-IR spectra of MTF@As NPs are thought to be caused by the attachment of metformin to the surface of the nanoparticles after the synthesis of NPs by microwave irradiation.

As a result of a quantitative analysis, each mg of prepared MTF@As NPs contained $18.6 \pm 0.3\text{ }\mu\text{g}$ of metformin. For other nanostructures like umbelliprenin-coated Fe_3O_4 NPs [47] and Fe_3O_4 @piroctone olamine NPs [48], it has been measured that each 1 mg of dried nanoparticles containing $250\text{ }\mu\text{g}$ of umbelliprenin, and $50\text{ }\mu\text{g}$ of piroctone olamine, respectively. Different factors like the chemical structure of the coated compound, type, size, shape, and synthesis method of nanoparticles could alter the quantitative of the coating process.

Antioxidant activity

Antioxidants can combat cancer development by delaying, preventing, and removing oxidative damage from Reactive oxygen species (ROS) [49]. This study aimed to evaluate the antioxidant activity of MTF@As NPs, As NPs, and an Ascorbic acid solution by measuring their DPPH scavenging activity and reducing power. This study aimed to calculate the antioxidant capacity of MTF@As NPs, As NPs, and Ascorbic acid solution by measuring their DPPH scavenging activity and iron-reducing power (Fig. 5a, b). A range of concentrations between $20\text{ }\mu\text{g/mL}$

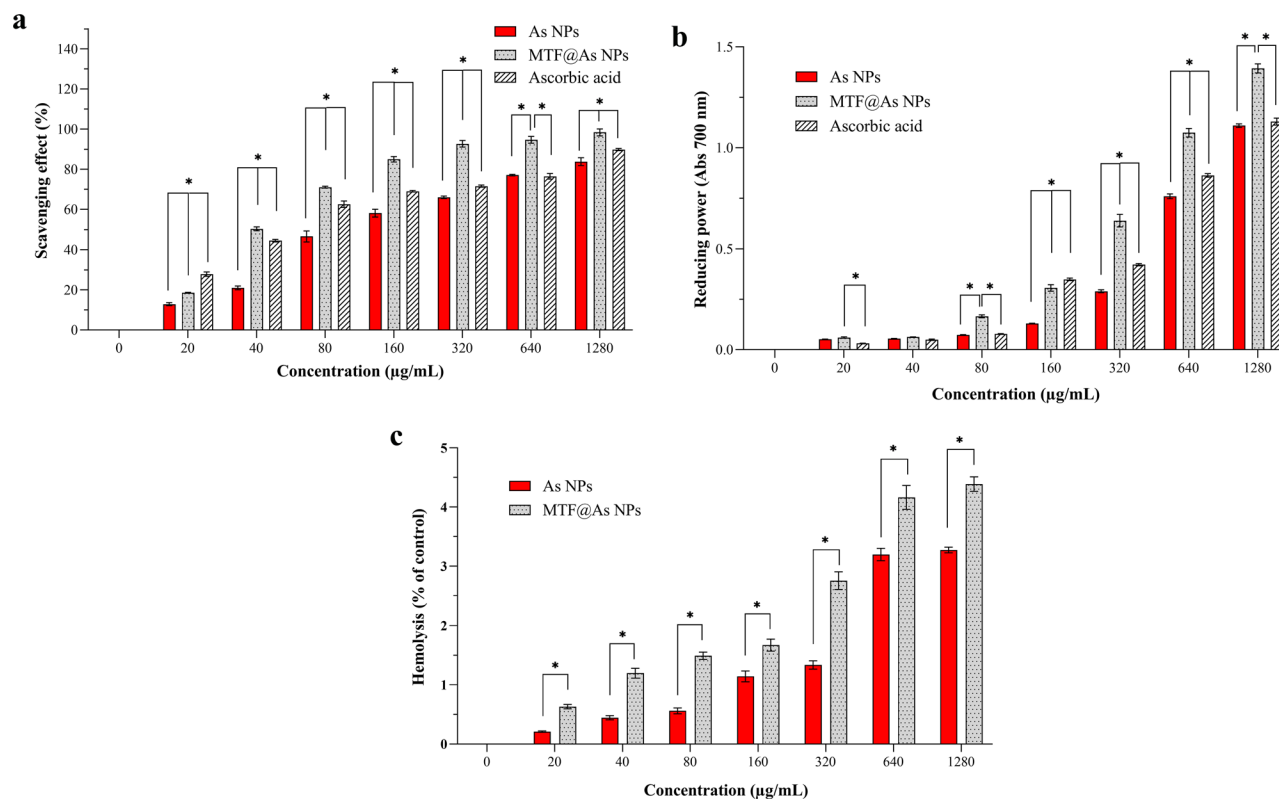


Fig. 5 The antioxidant activity of As NPs, MTF@As NPs, and Ascorbic acid was evaluated using (a) the DPPH-free radical scavenging and (b) Iron-reducing power (FRAP) methods, and (c) Hemolysis (%) caused by different concentrations of As NPs, MTF@As NPs. Data represented as mean \pm SD of three experiments (P -value < 0.05 was considered significant (*))

to 1280 µg/mL showed significantly greater scavenging activities with MTF@As NPs than As NPs and Ascorbic acid ($p < 0.05$). On the other hand, the study found that the scavenging effect of ascorbic acid at concentrations ranging from 20 µg/mL to 1280 µg/mL was significantly lower than the scavenging effect of MTF@As NPs ($p < 0.05$). This finding underscores the potential of MTF@As NPs as a promising antioxidant agent for various applications. Moreover, the scavenging effect of As NPs was significantly lower than that of Ascorbic acid at concentrations from 20 µg/mL to 1280 µg/mL ($p < 0.05$). The study found that the antioxidant activity of both MTF@As NPs and As NPs was dose administered. Previous studies have also reported that metformin's DPPH radical scavenging effect is concentration-dependent, with an IC_{50} value of 56.9 µg/ml. In comparison, the IC_{50} value of standard Ascorbic acid is 51.8 µg/ml [50]. Furthermore, higher DPPH scavenging activity has been observed in other complexes containing metformin than free metformin. For instance, Refat et al. reported that a metformin complex with cobalt is more effective as a free radical scavenger and has higher anti-tumor activity than free metformin [51].

The reducing power of MTF@As NPs, As NPs, and Ascorbic acid solution was measured by reducing Fe^{3+}

to Fe^{2+} ions (Fig. 5b). The reduction power of MTF@As NPs was greater than As NPs at concentrations from 80 to 1280 g/mL ($p < 0.05$). While Ascorbic acid had significantly higher reducing power than MTF@As NPs and As NPs at 160 µg/mL, MTF@As NPs had significantly higher reducing power than Ascorbic acid at concentrations > 320 g/mL ($p < 0.05$). (Fig. 5b). A large surface area or chemical structure on the surface of MTF@As NPs might contribute to the higher reducing power activity of the NPs. The higher reducing power activity of MTF@As NPs may be due to the chemical structure on the surface of NPs or the large surface area of NPs, which could reduce Fe^{3+} ions. The biosynthesis of microwave-irradiated insoluble Zn NPs (30–80 nm) has been reported to have a similar effect with higher reducing power activity than that of soluble Zn^{2+} ions [39].

The hemolytic properties of NPs

Based on the data in Fig. 5c, the study evaluated the percentage of hemolysis caused by MTF@As NPs and As NPs at varying concentrations. As a result of the hemolytic test, MTF@As NPs had a significantly higher hemolytic potential (HP) than As NPs at all concentrations tested ($p < 0.05$). According to the ASTM F 756-08 standard, materials exhibiting a hemolysis rate (HR) below

2% are categorized as non-hemolytic, while biomaterials are allowed an HR of up to 5% [52, 53]. MTF@As NPs/As NPs concentrations were dose-dependently related to hemolytic properties (HP). Mahmud et al. reported that exposure to arsenic trioxide activates erythrocyte phospholipid scrambling, leading to anemia by accelerating erythrocyte clearance from circulating blood [54]. Wang et al. reported that chemically synthesized round $\text{As}_2\text{O}_3/\text{Fe}_2\text{O}_3$ nanoparticles (100 nm) demonstrated an HP of 0.77%, which falls below the established threshold of 5%, indicating desirable compatibility with RBCs [55].

Cytotoxic activity

The cytotoxic properties of MTF@As NPs, As NPs, As_2O_3 , and metformin on MCF-7 and NIH3T3 cells were measured after 24 h of treatment (Fig. 6). The necessary concentration for the death of half of the cells (IC_{50}) for MCF-7 cells treated (24 h) with MTF@As NPs, As NPs, As_2O_3 , and metformin was measured to be 33.5 ± 2.6 $\mu\text{g}/\text{mL}$, 45.3 ± 1 $\mu\text{g}/\text{mL}$, 44.2 ± 3.8 $\mu\text{g}/\text{mL}$, and more than 1280 $\mu\text{g}/\text{mL}$, respectively. Furthermore, the IC_{50} for 3T3 cells treated (24 h) with MTF@As NPs, As NPs, As_2O_3 , and metformin was 5.7 ± 0.3 $\mu\text{g}/\text{mL}$, 15 ± 1.6 $\mu\text{g}/\text{mL}$, 11.8 ± 1.1 $\mu\text{g}/\text{mL}$, and more than 1280 $\mu\text{g}/\text{mL}$, respectively.

In concentrations ranging from 40 to 640 $\mu\text{g}/\text{mL}$, MTF@As NPs exhibited more significant cytotoxic effects on the MCF-7 cells than As NPs after 24 h (Fig. 6a). Moreover, As_2O_3 caused significantly more toxicity on MCF-7 cells when applied at concentrations between 160 and 640 $\mu\text{g}/\text{mL}$ compared to MTF@As NPs ($p < 0.05$). MTF@As NPs also exhibited significantly greater cytotoxicity than As NPs at concentrations of 10 $\mu\text{g}/\text{mL}$ and 20 $\mu\text{g}/\text{mL}$ after 24 h of exposure on 3T3 cells ($p < 0.05$) (Fig. 6b).

In the presence of studied concentrations (10–640 $\mu\text{g}/\text{mL}$), metformin showed significantly lower cytotoxic effects on MCF-7 and 3T3 cells than MTF@As NPs, As NPs, and As_2O_3 ($p < 0.05$). At concentrations between 10 and 640 $\mu\text{g}/\text{mL}$, the MTF@As NPs, and As_2O_3 exhibited significantly higher toxicity on the 3T3 cell line than on MCF-7 cells ($p < 0.05$). It should also be noted that the cytotoxicity of As NPs on 3T3 cells was more significant than that on MCF-7 cells ($p < 0.05$). In another study, As_4S_4 nanostructures with a size of 227 nm were synthesized using the wet nano-milling procedure. The cytotoxicity effect of these nanostructures against two multiple myeloma cell lines, RPMI-LR5 and OPM1 was evaluated. The nanostructures' half-maximal inhibitory concentration (IC_{50}) values were 0.57 $\mu\text{g}/\text{mL}$ and 0.21 $\mu\text{g}/\text{mL}$ for RPMI-LR5 and OPM1 cells, respectively [56]. Furthermore, As_4S_4 nano-suspensions of 137 nm and 153 nm showed potent cytotoxicity towards H460 human lung cancer cells, with an IC_{50} value of 0.031 μg and 0.066 μg ,

respectively. The induction of apoptosis in H460 cells by the nano-suspensions was confirmed by DNA damage and cell cycle arrest at G2/M and SubG1 phases [57]. As_2O_3 nanoparticles (10–40 nm) carried higher cytotoxicity, apoptosis rates, and downregulated B-cell lymphoma 2 expressions in acute promyelocytic leukemia cells (APL) than arsenic trioxide [16]. According to Jadhav et al., As_2O_3 nanostructures (75 nm) coated with dimercaptosuccinic acid and chitosan reduced the viability of mouse fibroblasts NIH-3T3 and prostate cancer cell lines (LNCaP and PC-3) more than uncoated As_2O_3 NPs (45 nm) [58]. Furthermore, human serum albumin-functionalized As_2O_3 nanoparticles (20 ± 2 nm) showed enhanced cytotoxicity against MCF-7 breast cancer cells compared to As_2O_3 alone. The mechanism of cytotoxicity involved increased superoxide dismutase activity and apoptosis induction [59]. In a previous study, arsenic trioxide and sodium arsenite-induced apoptosis in human leukemia HL-60 and human immortalized myelogenous leukemia K562 cells [60]. The apoptotic effect reduced HTERT and WT1 mRNAs and proteins while par-4 levels were increased. However, both cell lines expressed high levels of anti-apoptotic gene bcl-2 expression at low arsenic concentrations (0.1 mM). The authors suggested that par-4 upregulation might be more critical for apoptosis induction than bcl-2 downregulation [60]. According to Wang et al., arsenic trioxide treatment induces apoptosis in MCF-7 human breast cancer cells by triggering caspase-3 and decreasing HERG expression [61].

Arsenic-containing compounds can inhibit mitochondrial proteins by forming disulfide bonds between adjacent thiol groups, increasing the production of ROS and activating apoptotic signaling pathways. The level of transport systems that affect the uptake or removal of these compounds from cells and the level of redox defense mechanisms in the cells determine the sensitivity of cancer cells to these compounds [62]. Several factors can affect the toxicity mechanisms of cells treated with arsenic-containing nanostructures, including the shape, size, chemical composition, and nanoparticle preparation method. According to a study by Yang et al., the anti-hepatocellular carcinoma effects of arsenic trioxide were enhanced by metformin in HepG2 and BEL7402 cell lines. By reducing Bcl-2 expression, this anti-cancer effect was achieved [63]. As reported by Ling et al., metformin inhibits mitochondrial complex I to reduce the hepatotoxic effects of arsenic trioxide in AML12 cells [36]. The protective effects of metformin on arsenic trioxide-induced apoptosis were not due to metformin's inhibition of mitochondrial respiratory chain complex I. Metformin increased the intracellular NADH/NAD⁺ ratio, leading to decreased intracellular ROS induced by arsenic trioxide [36]. As reported in another study, metformin enhances the efficacy of arsenic trioxide in suppressing intrahepatic

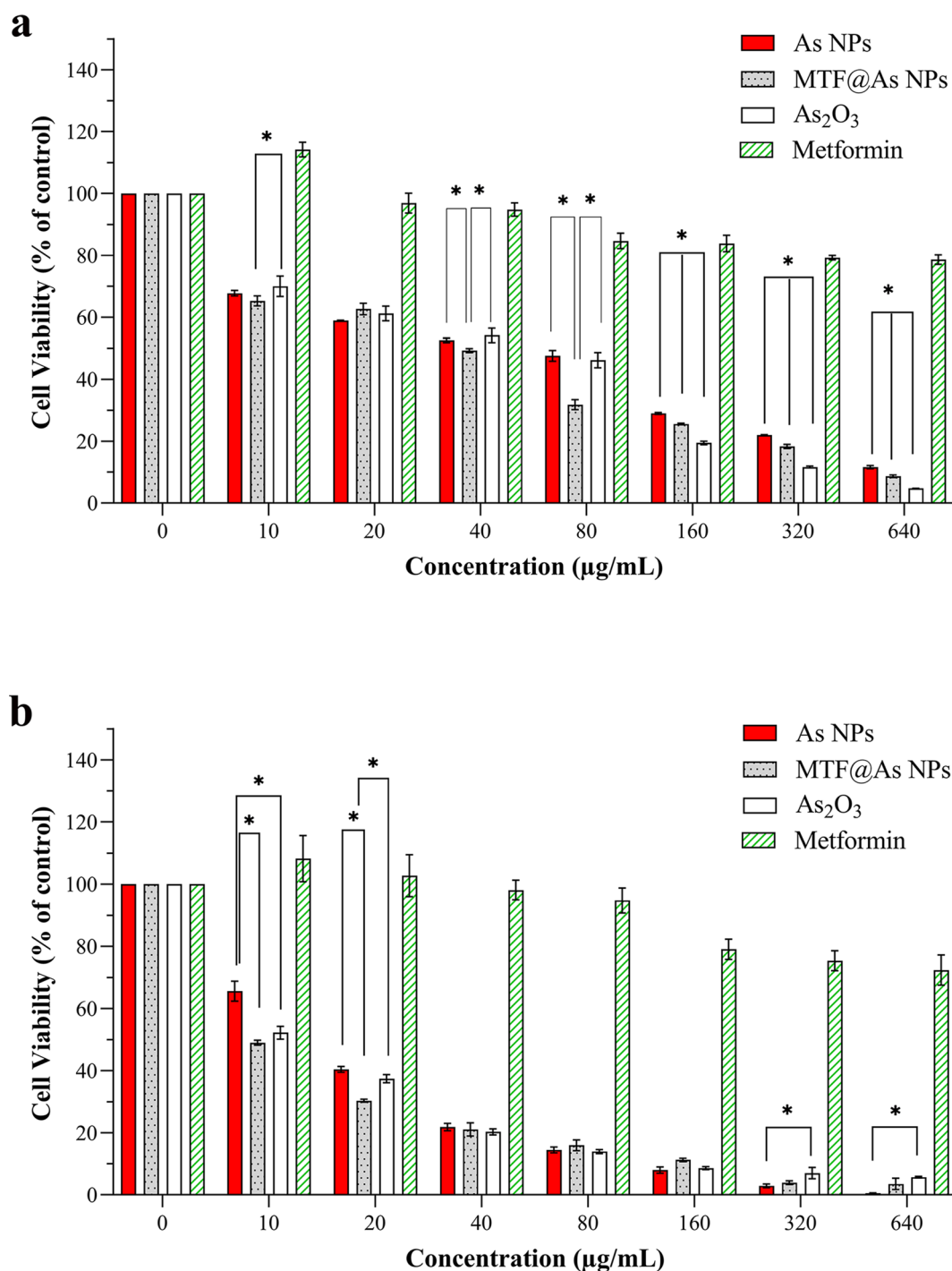


Fig. 6 Cytotoxicity effect of As NPs, MTF@As NPs, arsenic trioxide (As₂O₃), and metformin on (a) MCF-7 and (b) NIH3T3 cell lines using MTT assay after 24 h incubation at 37 °C with 5% CO₂. Metformin showed significantly lower cytotoxic effects on MCF-7 and 3T3 cells than MTF@As NPs, As NPs, and As₂O₃ ($p < 0.05$). All data represented as mean \pm SD of three experiments on different days (P -value < 0.05 considered as *)

cholangiocarcinoma via the AMPK/p38 MAPK-ERK3/mTORC1 pathway [37]. As a result of metformin and arsenic trioxide working in concert, mTORC1 is inhibited, AMPK is activated, and ERK3 is increased. Cell proliferation was inhibited by overexpression of EKR3 in cholangiocarcinoma cells by inhibiting mTORC1 [37].

As reported by Chen et al. in 2021, metformin augmented the effect of arsenic trioxide in preventing cell proliferation while promoting apoptosis in HeLa cells by activating Bax/Bcl-2-related [30]. In HeLa cells treated with arsenic trioxide, metformin also increased

autophagosome accumulation, stimulated the conversion of LC3-I to LC3-II, and decreased p62 levels.

metformin decreased mitochondrial membrane potential and activated the TOM system and PINK1/Parkin signaling pathways, increasing mitophagy and mitophagic apoptosis. As a consequence of these findings, HeLa cells are induced to undergo mitophagy in response to Further, metformin and arsenic trioxide, indicating that metformin synergizes with arsenic trioxide to induce cell death in a Parkin/PINK1-dependent mechanism [30]. Indeed, the exact mechanisms underlying the cytotoxic effects of MTF@As NPs have not been fully understood, and further research is needed to elucidate these mechanisms.

Conclusion

As a result of this study, MTF@As NPs demonstrated remarkable potential as a novel nanoparticle with significant cytotoxicity on the MCF-7 cell line. The findings provide valuable insight into the physicochemical properties and demonstrate their superior antioxidant activity compared to As NPs. Additionally, the study highlights the compatibility of MTF@As NPs with human RBCs, which is a critical factor for their potential use in medical applications. The study's results also reveal the promising cytotoxic effects of MTF@As NPs against MCF-7 and NIH3T3 cells. The superior performance of MTF@As NPs makes them a promising candidate for therapeutic and biomedical applications. Further research is needed to further investigate these nanoparticles' underlying mechanisms and potential applications. This study represents a significant step towards developing new and effective nanomedicines to combat various diseases.

Abbreviations

As NPs	Arsenic Nanoparticles
MTF@As NPs	Arsenic Nanoparticles containing Metformin
FTIR	Fourier transform infrared spectroscopy
EDS	Energy-dispersive X-ray spectroscopy
SEM	Scanning electron microscopy
XRD	X-ray diffraction
ATO	Arsenic trioxide
ROS	Reactive oxygen species
PLGA	Poly(lactide-co-glycolide)
APL	Acute promyelocytic leukemia
DPPH	Na ₂ HAsO ₄ ·7H ₂ O, 2,2-diphenyl-1-picrylhydrazyl
TCA	Trichloro acetic acid
MTT	3-(4, 5-dimethylthiazol-2-yl)-2, 5-diphenyl-2 H-tetrazolium bromide

Acknowledgements

We thank the Pharmaceutical Sciences and Cosmetic Products Research Center, Kerman University of Medical Sciences (Kerman, Iran), for their support (Grant number: 400001142).

Author contributions

All authors contributed and assisted in the completion of this study. M.SH. supervised, received the grant, and wrote the first draft of the manuscript. S.S.H. and S.R.M. synthesized and characterized the nanoparticles. M.A.S. accomplished cytotoxicity assay, interpreted results, and wrote the first draft in collaboration with M.SH. F.J.M. did hemolysis and antioxidant studies. H.F.R.

revised the results and edited the final version of the manuscript. All authors reviewed the manuscript.

Funding

This study was supported by the Pharmaceutical Sciences and Cosmetic Products Research Center, Kerman University of Medical Sciences (Kerman, Iran), for their support (Grant number: 400001142).

Data availability

All data involved in this study are presented in this article. The raw data of our study are available from the corresponding author on reasonable request.

Declarations

Ethics approval and consent to participate

This study was approved by the ethical committee of Kerman University of Medical Sciences (Ethical approval Code: IR.KMU.REC.1400.675).

Consent for publication

Not applicable.

Competing interests

The authors declare no competing interests.

Received: 12 May 2024 / Accepted: 11 February 2025

Published online: 28 March 2025

References

1. Rong Y, Dong F, Zhang G, Tang M, Zhao X, Zhang Y, et al. The crosstalk of lactate-histone lactylation and tumor. *Proteom – Clin Appl*. 2023. <https://doi.org/10.1002/prca.202200102>.
2. Yeşildağ A, Kızıloğlu HT, Dirican E, Erbaş E, Gelen V, Kara A. Anticarcinogenic effects of Gold nanoparticles and Metformin Against MCF-7 and A549 cells. *Biol Trace Elem Res*. 2024. <https://doi.org/10.1007/s12011-024-04090-y>.
3. Genchi G, Lauria G, Catalano A, Carocci A, Sinicropi MS. Arsenic: a review on a great health issue worldwide. *Appl Sci*. 2022. <https://doi.org/10.3390/app12126184>.
4. Paul NP, Galván AE, Yoshinaga-Sakurai K, Rosen BP, Yoshinaga MJB. Arsenic in medicine: past, present and future. *Biomaterials*. 2023. <https://doi.org/10.1007/s10534-022-00371-y>.
5. Vergara-Gerónimo CA, Del Río AL, Rodríguez-Dorantes M, Ostrosky-Wegman P, Salazar AM. Arsenic-protein interactions as a mechanism of arsenic toxicity. *Toxicol Appl Pharmacol*. 2021. <https://doi.org/10.1016/j.taap.2021.115738>.
6. Yang Y, Li Y, Li R, Wang Z. Research progress on arsenic, arsenic-containing medicinal materials, and arsenic-containing preparations: clinical application, pharmacological effects, and toxicity. *Front Pharmacol*. 2024. <https://doi.org/10.3389/fphar.2024.1338725>.
7. Chen J, Chen S, Luo H, Wu W, Wang S. The application of arsenic trioxide in cancer: an umbrella review of meta-analyses based on randomized controlled trials. *J Ethnopharmacol*. 2023. <https://doi.org/10.1016/j.jep.2023.116734>.
8. Wang QQ, Hua HY, Naranmandura H, Zhu H-H. Balance between the toxicity and anticancer activity of arsenic trioxide in treatment of acute promyelocytic leukemia. *Toxicol Appl Pharmacol*. 2020. <https://doi.org/10.1016/j.taap.2020.115299>.
9. Rehan F, Zhang M, Fang J, Greish K. Therapeutic applications of Nanomedicine: recent developments and future perspectives. *Molecules*. 2024. <https://doi.org/10.3390/molecules29092073>.
10. Al-Jubori AA, Sulaiman GM, Tawfeeq AT, Mohammed HA, Khan RA, Mohammed SA. Layer-by-layer nanoparticles of tamoxifen and resveratrol for dual drug delivery system and potential triple-negative breast cancer treatment. *Pharmaceutics*. 2021. <https://doi.org/10.3390/pharmaceutics13071098>.
11. Greish K. Recent and future advances in anticancer drug delivery: an interview with Khaled Greish. *Therapeutic Delivery*. 2018. <https://doi.org/10.4155/tde-2018-0019>.
12. Alenazi F, Saleem M, Khaja ASS, Zafar M, Alharbi MS, Hagbani TA, et al. Metformin encapsulated gold nanoparticles (MTF-GNPs): a promising antiangiogenic agent. *Cell Biochem Function*. 2022. <https://doi.org/10.1002/cbf.3738>.

13. Subastri A, Arun V, Sharma P, Preedia babu E, Suyavaran A, Nithyananthan S, et al. Synthesis and characterisation of arsenic nanoparticles and its interaction with DNA and cytotoxic potential on breast cancer cells. *Chemico-Biol Interact.* 2018. <https://doi.org/10.1016/j.cbi.2017.12.025>.
14. Covarrubias AA, Reyna-Jeldes M, Pedroso-Santana S, Marín S, Madero-Mendoza C, Demergasso C, et al. Arsenic nanoparticles trigger apoptosis via Anoikis Induction in OECM-1 cells. *Int J Mol Sci.* 2024. <https://doi.org/10.3390/ijms25126723>.
15. Salmani-Javan E, Jafari-Gharabaghlu D, Bonabi E, Zarghami N. Fabricating niosomal-PEG nanoparticles co-loaded with metformin and silibinin for effective treatment of human lung cancer cells. *Front Oncol.* 2023. <https://doi.org/10.3389/fonc.2023.1193708>.
16. Dong X, Ma N, Liu M, Liu Z. Effects of As₂O₃ nanoparticles on cell growth and apoptosis of NB4 cells. *Exp Ther Med.* 2015. <https://doi.org/10.3892/etm.2015.2651>.
17. Rabea S, Suliman K, Qian B, Hongmin L, Muhammad Wajid U, Mengzhou X. Arsenic Trioxide-based Nanomedicines as a Therapeutic Combination Approach for treating gliomas: a review. *Curr Nanosci.* 2021. <https://doi.org/10.2174/1573413716999201207142810>.
18. Hu J, Dong Y, Ding L, Dong Y, Wu Z, Wang W, et al. Local delivery of arsenic trioxide nanoparticles for hepatocellular carcinoma treatment. *Signal Transduct Target Therapy.* 2019. <https://doi.org/10.1038/s41392-019-0062-9>.
19. Fan L, Liu C, Hu A, Liang J, Li F, Xiong Y, et al. Dual oligopeptides modification mediates arsenic trioxide containing nanoparticles to eliminate primitive chronic myeloid leukemia cells inside bone marrow niches. *Int J Pharm.* 2020. <https://doi.org/10.1016/j.ijpharm.2020.119179>.
20. Song X, Wu J, Song W, Chen L, Zhang S, Ji H, et al. Thiolated chitosan nanoparticles for stable delivery and smart release of As₂O₃ for liver cancer through dual actions. *Carbohydr Polym.* 2023. <https://doi.org/10.1016/j.carbpol.2022.120462>.
21. Ferraro G, Pratesi A, Cirri D, Imbimbo P, Maria Monti D, Messori L, et al. Arsenoplatin-ferritin nanocage: structure and cytotoxicity. *Int J Mol Sci.* 2021. <https://doi.org/10.3390/ijms22041874>.
22. Su J, Liu G, Lian Y, Kamal Z, Que X, Qiu Y, et al. Preparation and characterization of erythrocyte membrane cloaked PLGA/arsenic trioxide nanoparticles and evaluation of their in vitro anti-tumor effect. *RSC Adv.* 2018. <https://doi.org/10.1039/c8ra01417e>.
23. Song X, Wang J, Xu Y, Shao H, Gu J. Surface-modified PLGA nanoparticles with PEG/LA-chitosan for targeted delivery of arsenic trioxide for liver cancer treatment: inhibition effects enhanced and side effects reduced. *Colloids Surf B.* 2019. <https://doi.org/10.1016/j.colsurfb.2019.04.036>.
24. Yin X-B, Wu L-Q, Fu H-Q, Huang M-W, Wang K, Zhou F, et al. Inhibitory effect of humanized anti-VEGFR-2 ScFv-As₂O₃-stealth nanoparticles conjugate on growth of human hepatocellular carcinoma: in vitro and in vivo studies. *Asian Pac J Trop Med.* 2014. [https://doi.org/10.1016/S1995-7645\(14\)60052-3](https://doi.org/10.1016/S1995-7645(14)60052-3).
25. Hernández-Velázquez ED, Alba-Betancourt C, Alonso-Castro AJ, Ortiz-Alvarado R, López JA, Meza-Carmen V, et al. Metformin, a biological and synthetic overview. *Bioorg Med Chem.* 2023. <https://doi.org/10.1016/j.bmc.2023.129241>.
26. Foretz M, Guigas B, Viollet B. Metformin: update on mechanisms of action and repurposing potential. *Nat Rev Endocrinol.* 2023. <https://doi.org/10.1038/s41574-023-00833-4>.
27. Pedrosa AR, Martins DC, Rizzo M, Silva-Nunes J. Metformin in SARS-CoV-2 infection: a hidden path—from altered inflammation to reduced mortality. A review from the literature. *J Diabetes Complicat.* 2023. <https://doi.org/10.1016/j.jdiacomp.2022.108391>.
28. Şeylan C, Tarhan Ç. Metformin extends the chronological lifespan of fission yeast by altering energy metabolism and stress resistance capacity. *FEMS Yeast Res.* 2023. <https://doi.org/10.1093/femsyr/foad018>.
29. Dankner R, Agay N, Olmer L, Murad H, Keinan Boker L, Balicer RD, et al. Metformin Treatment and Cancer Risk: Cox Regression Analysis, with Time-Dependent covariates, of 320,000 persons with Incident Diabetes Mellitus. *Am J Epidemiol.* 2019. <https://doi.org/10.1093/aje/kwz157>.
30. Chen J, Zhou C, Yi J, Sun J, Xie B, Zhang Z, et al. Metformin and arsenic trioxide synergize to trigger Parkin/pink1-dependent mitophagic cell death in human cervical cancer HeLa cells. *J Cancer.* 2021. <https://doi.org/10.7150/jca.61299>.
31. Wu X-y, Xu W-W, Huan X-k, Wu G-n, Li G, Zhou Y-H, et al. Mechanisms of cancer cell killing by metformin: a review on different cell death pathways. *Mol Cell Biochem.* 2023. <https://doi.org/10.1007/s11010-022-04502-4>.
32. Mlicka A, Mlicki P, Niewiadomski P, Zielińska W, Hałas-Wiśniewska M, Izdebska M. Synergistic effect of metformin and doxorubicin on the metastatic potential of T24 cells. *Acta Histochem.* 2023. <https://doi.org/10.1016/j.acthis.2022.151975>.
33. Mariana Nunes DD, Nuno Vale. Sara Ricardo the Antineoplastic Effect of Carboplatin is potentiated by combination with Pitavastatin or metformin in a Chemoresistant High-Grade Serous Carcinoma Cell line. *Int J Mol Sci.* 2023. <https://doi.org/10.3390/ijms24010097>.
34. Fatehi R, Rashedinia M, Akbarizadeh AR, Firouzabadi N. Metformin enhances anti-cancer properties of resveratrol in MCF-7 breast cancer cells via induction of apoptosis, autophagy and alteration in cell cycle distribution. *Biochem Biophys Res Commun.* 2023. <https://doi.org/10.1016/j.bbrc.2022.12.069>.
35. Cheng Y, Zhan P, Lu J, Lu Y, Luo C, Cen X, et al. Metformin synergistically enhances the antitumor activity of Lenvatinib in hepatocellular carcinoma by altering AKT-FOXO3 signalling pathway. *Liver Int.* 2023. <https://doi.org/10.1111/liv.15611>.
36. Ling S, Shan Q, Liu P, Feng T, Zhang X, Xiang P, et al. Metformin ameliorates arsenic trioxide hepatotoxicity via inhibiting mitochondrial complex I. *Cell Death Dis.* 2017. <https://doi.org/10.1038/cddis.2017.482>.
37. Ling S, Xie H, Yang F, Shan Q, Dai H, Zhuo J, et al. Metformin potentiates the effect of arsenic trioxide suppressing intrahepatic cholangiocarcinoma: roles of p38 MAPK, ERK3, and mTORC1. *J Hematol Oncol.* 2017. <https://doi.org/10.1186/s13045-017-0424-0>.
38. Forooutanfar H, Adeli-Sardou M, Nikkhoo M, Mehrabani M, Amir-Heidari B, Shahverdi AR, et al. Antioxidant and cytotoxic effect of biologically synthesized selenium nanoparticles in comparison to selenium dioxide. *J Trace Elem Med Biol.* 2014. <https://doi.org/10.1016/j.jtemb.2013.07.005>.
39. Salari Z, Ameri A, Forooutanfar H, Adeli-Sardou M, Jafari M, Mehrabani M, et al. Microwave-assisted biosynthesis of zinc nanoparticles and their cytotoxic and antioxidant activity. *J Trace Elem Med Biol.* 2017. <https://doi.org/10.1016/j.jtemb.2016.09.001>.
40. Satarzadeh N, Shakibaie M, Adeli-Sardou M, Jabari-Morouei F, Forooutanfar H, Sadeghi-Dousari A. Facile microwave-assisted biosynthesis of arsenic nanoparticles and evaluation their antioxidant properties and cytotoxic effects: a preliminary in vitro study. *J Clust Sci.* 2022. <https://doi.org/10.1007/s10876-022-02356-w>.
41. Pal A, Saha S, Kumar Maji S, Kundu M, Kundu A. Wet-chemical synthesis of spherical arsenic nanoparticles by a simple reduction method and its characterization. *Adv Mater Lett.* 2012. <https://doi.org/10.5185/amlett.2011.9305>.
42. Kalyan I, Pal T, Pal A. Time and temperature dependent formation of hollow gold nanoparticles via galvanic replacement reaction of as (0) and its catalytic application. *MRS Commun.* 2019. <https://doi.org/10.1557/mrc.2018.214>.
43. Edmundson MC, Horsfall L. Construction of a modular arsenic-resistance operon in *E. Coli* and the production of arsenic nanoparticles. *Front Bioeng Biotechnol.* 2015. <https://doi.org/10.3389/fbioe.2015.00160>.
44. Shakibaie M, Riahi-Madvar S, Ameri A, Amir-Moghadam P, Adeli-Sardou M, Forooutanfar H. Microwave assisted biosynthesis of cadmium nanoparticles: characterization, antioxidant and cytotoxicity studies. *J Clust Sci.* 2022. <https://doi.org/10.1007/s10876-021-02107-3>.
45. Ameri A, Shakibaie M, Rahimi H-R, Adeli-Sardou M, Raeisi M, Najafi A, et al. Rapid and facile microwave-assisted synthesis of palladium nanoparticles and evaluation of their antioxidant properties and cytotoxic effects against fibroblast-like (HSKMC) and human lung carcinoma (A549) cell lines. *Biol Trace Elem Res.* 2020. <https://doi.org/10.1007/s12011-019-01984-0>.
46. Shakibaie M, Torabi-Shamsabad R, Forooutanfar H, Amir-Moghadam P, Amirheidari B, Adeli-Sardou M, et al. Rapid microwave-assisted biosynthesis of platinum nanoparticles and evaluation of their antioxidant properties and cytotoxic effects against MCF-7 and A549 cell lines. *3 Biotech.* 2021. <https://doi.org/10.1007/s13205-021-03007-z>.
47. Khorramizadeh M, Esmail-Nazari Z, Zarei-Ghaane Z, Shakibaie M, Mollazadeh-Moghaddam K, Iranshahi M, et al. Umbelliprenin-coated Fe₃O₄ magnetite nanoparticles: antiproliferation evaluation on human fibrosarcoma cell line (HT-1080). *Mater Sci Eng C.* 2010. <https://doi.org/10.1016/j.msec.2010.05.005>.
48. Shakibaie M, Haghiri M, Jafari M, Amirpour-Rostami S, Ameri A, Forooutanfar H, et al. Preparation and evaluation of the effect of Fe₃O₄@piroctone olamine magnetic nanoparticles on matrix metalloproteinase-2: a preliminary in vitro study. *Appl Biochem Biotechnol.* 2014. <https://doi.org/10.1002/bab.1231>.
49. Azmanova M, Pitto-Barry A. Oxidative stress in cancer therapy: friend or enemy? *ChemBioChem.* 2022. <https://doi.org/10.1002/cbic.202100641>.
50. Nasrin F. Study of antimicrobial and antioxidant potentiality of anti-diabetic drug metformin. *Int J Pharm Drug Anal.* 2014; <https://www.ijpda.org/index.php/journal/article/view/46>

51. Refat MS, Kobeasy MI. Synthesis, spectroscopic, thermal, free radical scavenging ability, and antitumor activity studies of cobalt (II) metformin complex. *Russ J Gen Chem*. 2014. <https://doi.org/10.1134/S1070363214040288>.
52. Singh N, Sahoo SK, Kumar R. Hemolysis tendency of anticancer nanoparticles changes with type of blood group antigen: an insight into blood nanoparticle interactions. *Mater Sci Eng C*. 2020. <https://doi.org/10.1016/j.msec.2020.110645>.
53. Múzquiz-Ramos EM, Cortés-Hernández DA, Escobedo-Bocardo JC, Zugasti-Cruz A, Ramírez-Gómez XS, Osuna-Alarcón JG. In vitro and in vivo biocompatibility of apatite-coated magnetite nanoparticles for cancer therapy. *J Mater Sci Mater Med*. 2013. <https://doi.org/10.1007/s10856-013-4862-0>.
54. Mahmud H, Föllner M, Lang F. Arsenic-induced suicidal erythrocyte death. *Arch Toxicol*. 2009. <https://doi.org/10.1007/s00204-008-0338-2>.
55. Wang Z-Y, Song J, Zhang D-SJWW. Nanosized As₂O₃/Fe₂O₃ complexes combined with magnetic fluid hyperthermia selectively target liver cancer cells. *World J Gastroenterol*. 2009. <https://doi.org/10.3748/wjg.15.2995>.
56. Baláž P, Sedlák J, Pastorek M, Choluřová D, Vignarooban K, Bhosle S, et al. editors. In-vitro testing of Arsenic Sulfide nanoparticles for the treatment of multiple myeloma cells. *NSTI Nanotech*; 2011.
57. Bujňáková Z, Baláž P, Makreski P, Jovanovski G, Čaplovičová M, Čaplovič L, et al. Arsenic sulfide nanoparticles prepared by milling: properties, free-volume characterization, and anti-cancer effects. *J Mater Sci*. 2015. <https://doi.org/10.1007/s10853-014-8763-5>.
58. Jadhav V, Ray P, Sachdeva G, Bhatt P. Biocompatible arsenic trioxide nanoparticles induce cell cycle arrest by p21WAF1/CIP1 expression via epigenetic remodeling in LNCaP and PC3 cell lines. *Life Sci*. 2016. <https://doi.org/10.1016/j.lfs.2016.02.042>.
59. Das B, Rahaman H, Ghosh SK, Sengupta M. Synthesis and characterization of arsenic (III) oxide nanoparticles as potent inhibitors of MCF 7 cell proliferation through proapoptotic mechanism. *BioNanoScience*. 2020. <https://doi.org/10.1007/s12668-020-00726-0>.
60. Glienke W, Chow KU, Bauer N, Bergmann L. Down-regulation of wt1 expression in leukemia cell lines as part of apoptotic effect in arsenic treatment using two compounds. *Leuk Lymphoma*. 2006. <https://doi.org/10.1080/10428190600625398>.
61. Wang Y, Zhang Y, Yang L, Cai B, Li J, Zhou Y, et al. Arsenic trioxide induces the apoptosis of human breast cancer MCF-7 cells through activation of caspase-3 and inhibition of HERG channels. *Exp Ther Med*. 2011. <https://doi.org/10.3892/etm.2011.224>.
62. Ralph SJ. Arsenic-based antineoplastic drugs and their mechanisms of action. *Met-Based Drugs*. 2008. <https://doi.org/10.1155/2008/260146>.
63. Yang X, Sun D, Tian Y, Ling S, Wang L. Metformin sensitizes hepatocellular carcinoma to arsenic trioxide-induced apoptosis by downregulating Bcl2 expression. *Tumour Biol*. 2015. <https://doi.org/10.1007/s13277-014-2926-5>.

Publisher's note

Springer Nature remains neutral with regard to jurisdictional claims in published maps and institutional affiliations.